Biosensors and Bioelectronics 24 (2009) 2165–2170

Contents lists available at ScienceDirect

Biosensors and Bioelectronics

journal homepage: www.elsevier.com/locate/bios

Synergistically improved sensitivity for the detection of specific DNA sequences using polyaniline nanofibers and multi-walled carbon nanotubes composites

Tao Yang [a], Na Zhou [a], Yongchun Zhang [a], Wei Zhang [a], Kui Jiao [a,*], Guicun Li [b]

[a] Key Laboratory of Eco-Chemical Engineering (Ministry of Education), College of Chemistry and Molecular Engineering, Qingdao University of Science and Technology, No. 53 Zhengzhou Road, Qingdao 266042, China
[b] Key Laboratory of Nanostructured Materials, Qingdao University of Science and Technology, Qingdao 266042, China

ARTICLE INFO

Article history:
Received 11 August 2008
Received in revised form
14 November 2008
Accepted 17 November 2008
Available online 25 November 2008

Keywords:
Carbon nanotubes
Polyaniline nanofibers
Electrochemical DNA biosensor
PAT gene
NOS gene

ABSTRACT

A sensitive electrochemical DNA biosensor was successfully realized on polyaniline nanofibers (PANI), multi-walled carbon nanotubes (MWNT) and chitosan (CHIT) modified carbon paste electrode (CPE) based on the synergistic effect between PANI and MWNT nanoparticles in chitosan film. PANI and MWNT nanocomposites resulted in highly enhanced electron conductive and biocompatible nanostructured film, which was examined by scanning electron microscopy (SEM), cyclic voltammetry (CV) and electrochemical impedance spectroscopy (EIS). The immobilization of the probe DNA on the surface of electrode was largely improved due to the unique synergistic effect of PANI and MWNT. The DNA hybridization events were monitored with an EIS label-free detection strategy. Under the optimal conditions, the dynamic detection range of this DNA electrochemical biosensor was from 1.0×10^{-13} to 1.0×10^{-7} mol/L and a detection limit of 2.7×10^{-14} mol/L for the detection of DNA specific sequence of the phosphinothricin acetyltransferase gene (PAT, one of the important screening detection genes for the transgenic plants). Simultaneously, the polymerase chain reaction (PCR) amplification of the terminator of nopaline synthase gene (NOS) from the sample of one kind of genetically modified soybean was also detected satisfactorily.

1. Introduction

Polyaniline (PANI) is one of the most attractive conducting polymers because of its high conductivity, ease of preparation, good environmental stability and extensive applications, such as electrochemical analysis, catalysis, electronic devices and biosensors (Xue et al., 2005; Kalakodimi and Nowak, 2002; Gerard et al., 2002; Li et al., 2006). In recent years, many investigations have focused on PANI nanostructures. Compared with the traditional PANI, the nanostructured PANI has both the advantages described above and its unique merit of high surface area as nanomaterials (Anilkumar and Jayakannan, 2007; Virji et al., 2004; Zhang et al., 2006; Lee et al., 2006; Yang et al., 2007a; Zhang et al., 2005c). Therefore, with the introduction of PANI nanomaterials, the electrochemical biosensors could show excellent sensitivity and selectivity (Ma et al., 2006a; Chang et al., 2007; Feng et al., 2008). For instance, Luo reported that nanostructured polyaniline films were electrochemically prepared on the electrode modified with multilayers of polystyrene nanoparticles for the detection of nitrite (Luo et al., 2007). Zhu reported that an electrochemical DNA biosensor based on electrochemically fabricated polyaniline nanowire through a three-step electrochemical deposition procedure was applied for the DNA hybridization detection (Zhu et al., 2006). Zhou reported that a glucose biosensor based on the dispersion of platinum microparticles in nano-fibrous polyaniline exhibited good anti-interference ability to the detection of uric acid and ascorbic acid (Zhou et al., 2005).

On the other hand, tremendous efforts over the past decade have been made to prepare nanocomposites of conducting polymer and carbon nanotube with an aim to combine the merits of each individual component (Zhang and Gorski, 2005; Ajayan et al., 1994; Sainz et al., 2005). Among these nanocomposites, it would be interesting to develop PANI and carbon nanotube composites that revealed redox activity (Ma et al., 2006b; Wei et al., 2003; Nascimento et al., 2005; Zhang et al., 2005b; Gao et al., 2000) at neutral pH values due to the doping of PANI with anionic species (Granot et al., 2005; Raitman et al., 2002), and to examine their bioelectrochemical activation based on the synergistic effect (Zhang and Gorski, 2005; Ali et al., 2007; Zou et al., 2007; Zhang et al., 2004). Polyaniline (PANI)–Prussian Blue (PB)/multi-walled carbon nanotubes (MWNTs) hybrid nanocomposite with synergistic effect between the PANI–PB and MWNTs was reported to fabricate H_2O_2 and glucose biosensor (Zou et al., 2007). Zhang described a new electrode system that utilized synergy between carbon nanotubes and toluidine blue O (TBO) to facilitate electron-transfer processes and to be used for the oxidation of the enzyme cofactor

* Corresponding author. Fax: +86 532 84023927.
E-mail address: kjiao@qust.edu.cn (K. Jiao).

0956-5663/$ – see front matter © 2008 Elsevier B.V. All rights reserved.
doi:10.1016/j.bios.2008.11.011

nicotinamide adenine dinucleotide (NADH) (Zhang and Gorski, 2005).

Chitosan (CHIT) is an abundant natural biopolymer with excellent film forming ability, biocompatibility, nontoxicity, good water permeability, high mechanical strength and adhesion to the chemically modified fabrication (Lu et al., 2006; Rubianes and Rivas, 2007; Siqueira et al., 2006; Sorlier et al., 2001; Yang et al., 2006). Furthermore, as well known, MWNT functionalized with carboxylic groups are well dispersed in CHIT solution with good stability. Hence, biomembrane-like film based on PANI, MWNT and CHIT may provide a favorable microenvironment for biomolecules immobilized on the electrode surface and enhance electron transfer between biomolecule and electrodes in bioanalytical area.

Considering all of those described above, in the present investigation, we described the integration of PANI and MWNT in a CHIT film for fabricating electrochemical biosensor with improved sensitivity towards DNA detection. The PANI-MWNT/CHIT composites, which were prepared by simply dispersing a certain ratio of PANI-MWNT in CHIT solution, were modified on a carbon paste electrode (CPE) surface. The nanocomposites showed excellent properties through synergistic effects of the component materials. The conductivity and electrochemical activity of the modified electrode were greatly enhanced. The very large surface area of the composites greatly increased the loading of the DNA probe. The biosensor was applied to the sensitive detection of the DNA specific sequences of the transgenic genes in the genetically modified crops, such as the phosphinothricin acetyltransferase gene (PAT) and the terminator of nopaline synthase gene (NOS).

2. Experimental

2.1. Apparatus and reagents

A CHI 660C electrochemical analyzer (Shanghai CH Instrument Company, China), which was in connection with a home-made carbon paste modified working electrode (Φ = 4 mm), a saturated calomel reference electrode (SCE) and a platinum wire auxiliary electrode, was used for the electrochemical measurement. Scanning electron microscopy (SEM) was carried out using a JSM-5900 machine (JEOL, Japan). The polymerase chain reaction (PCR) amplification was performed by an Eppendorf Mastercycler Gradient PCR system (Germany). Aquapro ultrapure water system (Ever Young Enterprises Development. Co., Ltd., China).

Polyaniline nanofibers (PANI) were supplied from the Material College of Qingdao University of Science and Technology (Li and Zhang, 2004). Multi-walled carbon nanotubes (MWNT, purity >95%) (Shenzhen Nanotech Port Company, China). Chitosan (CHIT) (Shanghai Reagent Company). All the chemicals are of analytical grade and solutions were prepared with ultrapure water.

Materials for the detection of PAT gene were synthesized by Beijing SBS Gene Technology Limited Company. Their base sequences are listed below:

probe DNA (ssDNA): 5′-GCC ACA AAC ACC ACA AGA GT-3′
target DNA: 5′-ACT CTT GTG GTG TTT GTG GC-3′
one-base mismatched DNA: 5′-ACT CTG GTG GTG TTT GTG GC-3′
two-base mismatched DNA: 5′-ACT CTG GTG GTG CTT GTG GC-3′
ncDNA: 5′-CAT GGT TGA TCC GTT CGC TG-3′

Materials for the PCR amplification of NOS gene sample: one pair of primers (19-base for every primer). Primer 1 was also used as the NOS gene probe. Their base sequences are as below:

primer 1: 5′-ATC GTT CAA ACA TTT GGC A-3′
primer 2: 5′-ATT GCG GGA CTC TAT CAT A-3′

The DNA template of the NOS gene sample for PCR amplification was extracted from one kind of the genetically modified soybean according to the method of plant DNA mini prep kit (Shanghai Academy of Agricultural Sciences).

All oligonucleotides stock solutions of 20-base oligomers (1.0 μmol/L) were prepared using Tris–HCl solution (5.0 mmol/L Tris–HCl, 50.0 mmol/L NaCl, pH 7.0), which were stored at 4 °C. More diluted solutions were obtained via diluting aliquot of the stock solution with ultrapure water prior to use. The hybridization solution was diluted with 2× SSC, which was consisted of 0.30 mol/L NaCl and 30.0 mmol/L sodium citrate tribasic dihydrate ($C_6H_5Na_3O_7{\cdot}2H_2O$).

2.2. Procedure

2.2.1. Preparation of CPE and PANI-MWNT/CHIT/CPE

The fabrication of CPE was carried out using a method of Jiang et al. (2008). 1 mg MWNT was suspended in a 40 mL concentrated HCl/HNO_3 (3:1 v/v) mixture and sonicated in a water bath for 5 h, then filtered and washed with ultrapure water until the filtrate became neutral, and finally dried under vacuum. The purified MWNT (1 mg) was then dispersed into 1 mL ultrapure water. Then, 1 mL MWNT solution and 1 mL of 1 g/L polyaniline nanofibers solution were dispersed by sonication for 5 min. In this way, uniform PANI-MWNT composites could be successfully fabricated. Supplementary material, Fig. S1 showed the synthesis route of the PANI-MWNT composites. There was spontaneous interaction of the MWNT and PANI nanoparticles.

Then, MWNT and PANI nanocomposites were dispersed in 50 mL of 1 g/L CHIT solution. 5 μL of the mixed gelatin solution was dripped onto the fresh surface of the CPE and naturally dried in the air to form PANI-MWNT/CHIT/CPE.

2.2.2. Immobilization and hybridization of DNA

The immobilization of the DNA probe on the electrode surface was carried out with following procedure: The PANI-MWNT/CHIT/CPE was immersed in 2.0 mL Tris–HCl buffer solution (pH 7.0) containing 1.0 μmol/L probe DNA at room temperature for 1.5 h to adsorb the probe DNA, followed by washing the electrode with 0.2% sodium dodecyl sulfate (SDS) solution and then rinsing it with ultrapure water. Hybridization reaction was conducted by immersing the ssDNA/PANI-MWNT/CHIT/CPE into hybridization solution containing 1.0 μmol/L target DNA at 40 °C for 40 min. Then the electrode was washed with 0.2% SDS solution to remove the unhybridized DNA and this hybridized electrode was denoted as dsDNA/PANI-MWNT/CHIT/CPE.

2.2.3. PCR amplification of DNA template from genetically modified soybean

The amplification mixture, in a final volume of 25 μL, contained 12 pmol primer 1, 12 pmol primer 2, 2 mmol/L $MgCl_2$, 0.2 mmol/L dATP, 0.2 mmol/L dCTP, 0.2 mmol/L dGTP, 0.2 mmol/L dTTP, 1.5 U Taq DNA polymerase (Promega, WI, USA), DNA template (50 ng DNA), 10 × reaction buffer B (Promega, WI, USA) in a 0.2 mL reaction tube.

The PCR procedure comprised an initial denaturation at 94 °C for 3 min, followed by 40 amplification cycles. Each cycle consisted of annealing at 56 °C for 20 s, extension at 72 °C for 20 s, denaturation at 94 °C for 30 s. After 40 amplification cycles, an extension step was performed at 72 °C for 6 min.

The purification for the PCR amplification was carried out via agarose gel electrophoresis. A well of the reaction solution, which was added 5 μL of agarose gel loading dye, contained a 1.0% low-melting temperature agarose gel. Electrophoresis was carried out at 100–120 mA for 30–60 min, and then excised the desired band visualized under UV light with a clean razor blade. Then the Purifi-

cation kit was used (TIANgel Maxi purification kit DP210-02, Beijing, China) for purifying the DNA in the gel. The PCR amplification sample gave an A_{260}/A_{280} ratio of 1.82, indicating that the DNA was pure enough.

2.2.4. Electrochemical measurements

Cyclic voltammetry (CV) and differential pulse voltammetry (DPV) were used in the electrochemical measurement. The following parameters were employed for CV and DPV, respectively: CV: scan rate 100 mV/s; DPV: pulse amplitude 50 mV, pulse width 60 ms, pulse period 0.2 s. Supporting electrolyte was a 1.5×10^{-5} mol/L MB in a B-R buffer solution of pH 6.0 including 25.0 mmol/L NaCl or a 1.0 mmol/L $K_3[Fe(CN)_6]$ and 1.0 mmol/L $K_4[Fe(CN)_6]$ (1:1) solution containing 0.1 mol/L KCl. As for MB supporting electrolyte, the electrode was transferred into the solution to accumulate for 5 min before the measurement.

The electrochemical impedance spectroscopic measurements were also carried out with the CHI 660C electrochemical analyzer. Supporting electrolyte solution was 1.0 mmol/L $K_3[Fe(CN)_6]$ and 1.0 mmol/L $K_4[Fe(CN)_6]$ (1:1) solution containing 0.1 mol/L KCl. The AC voltage amplitude was 5 mV and the voltage frequencies range from 10 kHz to 0.1 Hz. The applied potential was 172 mV.

The reported result for every electrode in this paper was the mean value of three parallel measurements.

3. Results and discussion

3.1. The synergistic effects of PANI and MWNT in chitosan film

Steady-state CV measurements for the different modified CPE electrodes in 1.0 mmol/L $[Fe(CN)_6]^{3-/4-}$ containing 0.1 mol/L KCl were utilized to explore the synergistic effect of polyaniline nanomaterials and the multi-walled carbon nanotubes (see Supplementary material, Fig. S2A). The well-defined oxidation and reduction peaks due to the Fe^{3+}/Fe^{2+} redox couple were noticeable, respectively. The PANI-MWNT/CHIT/CPE exhibited the highest redox peaks. Its oxidation peak current was about 3.09 times larger than that of the PANI/CHIT film modified electrode and about 2.12 times larger than that of the MWNT/CHIT film modified electrode.

Additionally, to further explore the relative interaction mechanism, Nyquist diagrams of $[Fe(CN)_6]^{3-/4-}$ at different modified electrodes were illustrated (see Supplementary material, Fig. S2B). The electrochemical impedance spectroscopy (EIS) can give information on the impedance changes of the electrode surface during the modification processes (Jiang et al., 2008). The surface electron transfer resistance value, R_{et}, in the spectrum corresponds to the diameter of the semicircle. Compared with the MWNT/CHIT/CPE and PANI/CHIT/CPE, the PANI-MWNT/CHIT/CPE exhibited almost a straight line, which is the characteristic of a diffusion-controlled step. It could be attributed to that the presence of synergistic effects in PANI-MWNT/CHIT film further enlarged the conductivity of the modified electrode. In view of the observations, the synergistic effect of polyaniline nanomaterials with the multi-walled carbon nanotubes in the $[Fe(CN)_6]^{3-/4-}$ redox system had been clearly demonstrated.

3.2. Electrochemical characterization of DNA modified electrode

Methylene Blue (MB) is a well-known indicator of DNA biosensor. It is based on the affinity of MB for the guanine bases of DNA (Azar et al., 2006; Yang et al., 2008). Thus, the increased loading of ssDNA probe can enhance the signal response of MB. The differential pulse voltammetry of 1.5×10^{-5} mol/L MB at different kinds of modified electrodes were recorded (see Supplementary material, Fig. S3). Compared with the DPV of MB at ssDNA/PANI/CHIT/CPE and ssDNA/MWNT/CHIT/CPE, ssDNA/PANI-MWNT/CHIT/CPE had the largest signal response, which indicated the greatly enhanced immobilization of the DNA probe on the electrode surface as a result of the synergistic effects of PANI-MWNT/CHIT film.

The sensitivity of DNA hybridization assay is directly related to the surface coverage of DNA probes on the electrode, which can be evaluated by using the electrochemical signal of MB from its affinity for the guanine bases of DNA molecules (Yang et al., 2007b). In our experiments, the quantity of electric charge for MB was 3.036×10^{-5} C, obtained by integrating its cathodic peak area after the binding with the DNA probes on the PANI-MWNT/CHIT/CPE. The quantity of MB on the modified electrode surface was calculated to be 1.576×10^{-10} mol according to the equation: $N = Q/neN_A$, where N represents the quantity of MB; Q is the electric charge quantity for MB; n is the number of electrons participating in the reaction, $n = 2$ in this experiment; e is the charge quantity of one electron, which is 1.6×10^{-19} C; N_A represents Avogadro's number, and its value is 6.02×10^{23} mol^{-1}. One MB molecule can be combined with a guanine base, and every PAT ssDNA probe sequence contains three guanine bases. Therefore, the surface density of the DNA probes was calculated as the product of the amount of MB and the stoichiometric ratio of MB to the DNA probe (3:1). The surface density of DNA probes on the PANI-MWNT/CHIT/CPE surface (diameter 4 mm) was estimated to be 4.183×10^{-10} mol/cm^2.

Recently, label-free biosensor based on electrochemical impedance spectroscopy (EIS), which is more simple and convenient, has aroused widely attention in detecting immobilization and hybridization reaction of DNA (Peng et al., 2007; Katz et al., 2005).

Fig. 1 illustrated the results of impedance spectroscopy on different electrodes in 1.0 mmol/L $[Fe(CN)_6]^{3-/4-}$ solution containing 0.1 mol/L KCl. The electron transfer resistance (R_{et}) of PANI-MWNT/CHIT/CPE electrode (Fig. 1b) reduced enormously as compared with that of the bare CPE electrode (Fig. 1a) due to the enhanced conductivity and electrochemical activity of composites-film. An increase of R_{et} value (Fig. 1c) was observed for the ssDNA/PANI-MWNT/CHIT/CPE electrode that obtained by immersing the PANI-MWNT/CHIT/CPE into 1.0 μmol/L probe DNA solution at room temperature for 1.5 h. The reason was that the immobilized DNA films generated a negative charge surface, repelling $[Fe(CN)_6]^{3-/4-}$. When the dsDNA/PANI-MWNT/CHIT/CPE electrode was finally fabricated after hybridization with the 1.0 μmol/L target DNA at 40 °C for 40 min, the R_{et} value increased largely (Fig. 1d). This may be owing to the following two reasons: more negative charges on the electrode surface and thicker DNA modified layer.

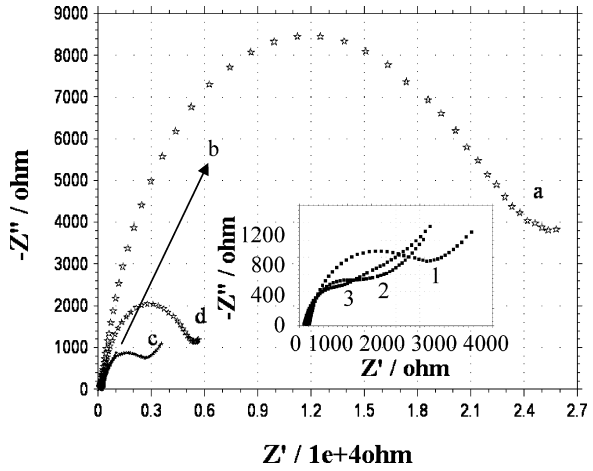

Fig. 1. Nyquist plots recorded at (a) bare CPE, (b) PANI-MWNT/CHIT/CPE, (c) ssDNA/PANI-MWNT/CHIT/CPE, (d) dsDNA/PANI-MWNT/CHIT/CPE. (inset: (1) ssDNA/PANI-MWNT/CHIT/CPE, (2) ssDNA/PANI/CHIT/CPE, (3) ssDNA/MWNT/CHIT/CPE.). Supporting electrolyte solution is 1.0 mmol/L $K_4[Fe(CN)_6]/K_3[Fe(CN)_6]$ (1:1) in 1.0 mol/L KCl.

The inset of Fig. 1 displays the Nyquist plots of ssDNA/PANI/CHIT/CPE (1), ssDNA/MWNT/CHIT/CPE (2) and ssDNA/PANI-MWNT/CHIT/CPE (3). As can be seen, as compared with the signal obtained at the ssDNA/PANI/CHIT/CPE or ssDNA/MWNT/CHIT/CPE, the ssDNA/PANI-MWNT/CHIT/CPE offered a maximal signal. This confirmed the synergistic effects of PANI-MWNT/CHIT composite film, which could effectively increase the loading of the ssDNA probe, ascribed to the excellent electron-transfer ability of MWNT and the larger surface area of PANI and MWNT dispersed in CHIT film.

3.3. Optimization of experimental conditions

The morphologies and microstructures of the PANI nanofibers and PANI-MWNT nanocomposites under different ratios of PANI to MWNT were studied by field-emission scanning electron microscopy (SEM). Typical SEM images of polyaniline nanofibers were shown in Fig. 2A. It was clear that these polyaniline nanofibers were in the form of small bundles. The diameters of the polyaniline branches ranged from 30 to 60 nm, and the lengths were several hundred nanometers. The SEM images of PANI-MWNT nanocomposites for the ratios of PANI to MWNT as 1:0.01, 1:0.1, 1:1 and 1:2 were corresponding to Fig. 2B–E, respectively. From the images, when the ratio was 1:1 (Fig. 2D), the homogeneously dispersed PANI-MWNT nanocomposites could be observed and the surface area is the largest, and most of the nanocomposites were interconnected to form dendritic or network structures, which would be of benefit to the sensor performance because the well-dispersed nanocomposites were electrochemically accessible (Zhang et al., 2005a). However, when the ratio was 1:2, the most of PANI had been entrapped in the MWNT film (Fig. 2E).

Electrochemical behavior of the as-prepared different modified films were studied by cyclic voltammetry with $[Fe(CN)_6]^{3-/4-}$ as the redox couple. As shown in Fig. 3A, the CV redox peaks increased with the change of the ratio of PANI to MWNT from 1:0.01 to 1:1. A maximal CV signal was obtained with the ratio of 1:1. After that, the signal of 1:2 ratio decreased. The Nyquist plots were shown in Fig. 3B, which also showed that the minimum R_{et} value was obtained at the ratio 1:1. This ratio was selected in our experiments.

The adsorption time of the probe DNA was also optimized. The R_{et} values of the ssDNA/PANI-MWNT/CHIT/CPE and dsDNA/PANI-MWNT/CHIT/CPE for the probe DNA adsorption times of 0.5, 1.0, 1.5, 2.0 and 2.5 h, respectively, were compared. As the adsorption time increased, the difference of the impedance values (ΔR_{et}) between the two DNA modified electrodes rose gradually at first (up to 1.5 h) and then reached a constant level. Therefore, an adsorption time of 1.5 h was used in our experiments.

The hybridization temperature and hybridization time have important influence on the hybridization reaction. After the immobilization of the probe DNA under the optimal conditions, the ssDNA/PANI-MWNT/CHIT/CPE was hybridized by immersing it into a stirring hybridization solution including target DNA at different temperatures, such as 30, 33, 35, 37 40, 43, 45, 47, 50 and 60 °C, for different times, such as 10, 20, 30, 40, 50 and 60 min.

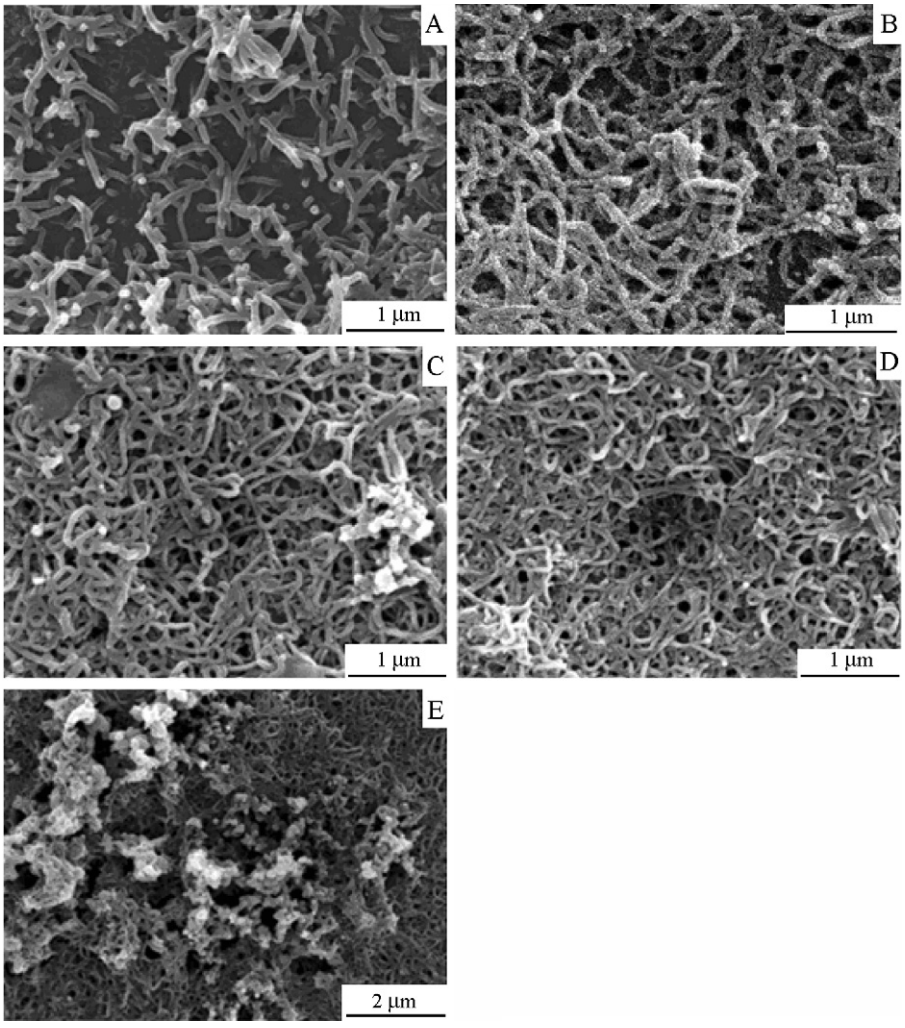

Fig. 2. SEM images of PANI nanomaterials (A) and PANI-MWNT nanocomposites film under different ratios of PANI to MWNT as 1:0.01 (B), 1:0.1 (C), 1:1 (D) and 1:2 (E).

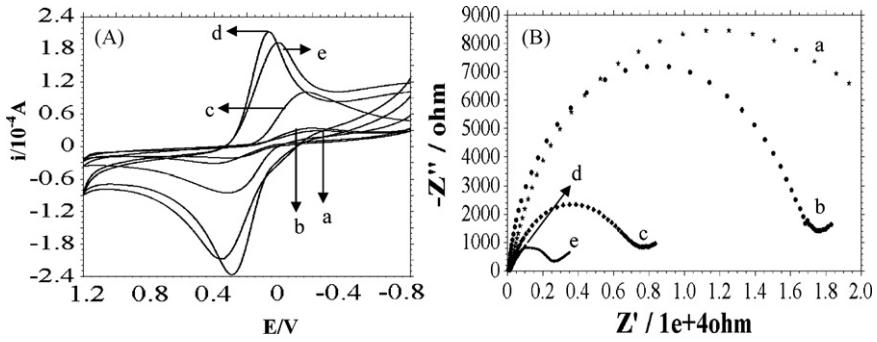

Fig. 3. Cyclic voltammograms (A) and Nyquist plots (B) of 1.0 mmol/L $K_4[Fe(CN)_6]/K_3[Fe(CN)_6]$ (1:1) in 0.1 mol/L KCl at (a) bare CPE and (b) 1:0.01; (c) 1:0.1; (d) 1:1; (e) 1:2 on the ratio of PANI:MWNT nanocomposites in CHIT film modified CPE.

The Nyquist plots of 1.0 mmol/L $[Fe(CN)_6]^{3-/4-}$ solution containing 0.1 mol/L KCl for every electrode before and after hybridization were recorded. The $R_{dsDNA} - R_{ssDNA}$ value (ΔR_{et}) versus the hybridization temperature was plotted (see supplementary material, Fig.S4, only shown 30, 40, 50 and 60 °C). The larger the ΔR_{et} value, the better the hybridization. The largest ΔR_{et} value was obtained when the hybridization was conducted at 40 °C for 40 min. Thus, the optimal hybridization temperature was selected as 40 °C and the optimal hybridization time as 40 min.

3.4. Detection of sequence-specific PAT gene fragment

The selectivity of the sensor was investigated by measuring the responses to different DNA hybridization sequences. Fig. 4 presents the normalized sensor response, $\Delta R_{et}/\Delta R^{o}_{et}$ ($\Delta R_{et} = R_{dsDNA} - R_{ssDNA}$, ΔR^{o}_{et} being the change in the electron transfer resistance when hybridized with complementary DNA), for the various targets. The responses to one-base mismatched, two-base mismatched, and fully noncomplementary DNA were 77.8%, 25.9% and 3.7% of the signal for the fully complementary DNA target, respectively. The diagram above showed the high selectivity of this biosensor.

The R_{et} value after the hybridization reaction showed an increase with increasing the cDNA concentration in the hybridization solution (see supplementary material, Fig.S5). The ΔR_{et} value was proportional to the logarithm of the sequence-specific DNA concentrations in the range from 1.0×10^{-13} mol/L to 1.0×10^{-7} mol/L and the linear regression equation is ΔR_{et} (Ω) = 434.50 log C + 5907.86 with a detection limit of 2.7×10^{-14} mol/L at a signal to noise ratio of 3σ (where σ is the standard deviation of a blank solution, $n = 11$) (RSD = 0.996). With the PANI-MWNT/CHIT films and a label-free detection using the electrochemical impedance spectroscopy, the sensitivity was greatly enhanced and the detection limit largely lowered for the DNA determination. At the same time, the detection range was very wide. Supplementary material, Table S1 listed the comparative results of the performances of this DNA biosensor with the previous reports regarding carbon nanotube-based composites systems.

3.5. Precision, regeneration and stability of DNA sensor

The regeneration of a DNA sensor is achieved by either a thermal or a chemical regeneration procedure. In this work, the regeneration ability of this DNA sensor was evaluated by denaturing the hybridized dsDNA on the electrode surface. The hybridized dsDNA electrode was denatured by immersing it into 10 mmol/L NaOH (2 min) (Li et al., 2007), followed by rinsing the electrode with the aquapro ultrapure water, and the regenerated probe DNA/PANI-MWNT/CHIT/CPE was used repetitively. The Nyquist diagrams of $[Fe(CN)_6]^{3-/4-}$ solution at the regenerated ssDNA/PANI-MWNT/CHIT/CPE and the hybridized dsDNA/PANI-MWNT/CHIT/CPE electrode were recorded. The results indicated that the two R_{et} values and ΔR_{et} value were, respectively, almost the same values as those obtained in the first experiment. Repetitive experiments showed that the DNA sensor could be reproduced for eight times without losing its sensitivity.

The stability of the DNA biosensor was tested. No significant changes in R_{et} value were observed after 24 h storage at 4 °C. After 10 days, the DNA probe could retain 92% of its initial sensitivity. Thus, the prepared DNA biosensor was suited for a stable platform for further quantitative measurements.

3.6. Qualitative analysis related to the PCR product of NOS gene

The NOS gene sample was also qualitatively detected by combining this electrochemical sensor with the PCR amplification

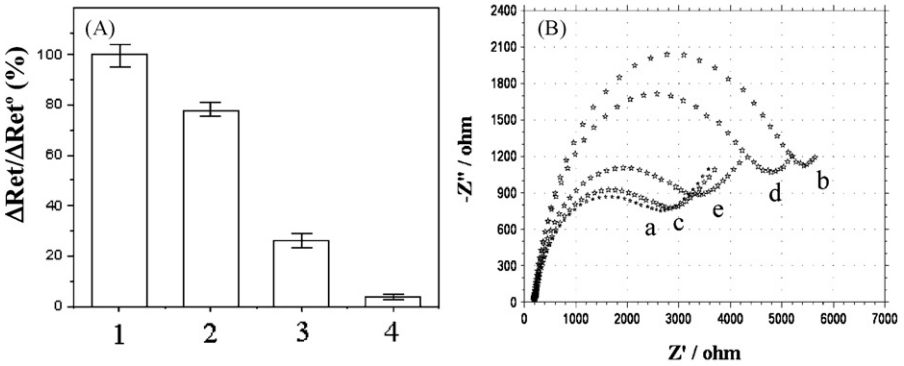

Fig. 4. (A) Normalized changes in the electron transfer resistance of a sensor based on PANI-MWNT/CHIT film after hybridization with different DNA sequences: 1. cDNA; 2. one-base mismatched DNA; 3. two-base mismatched DNA; 4. ncDNA. ΔR^{o}_{et} being the change in the electron transfer resistance when hybridized with complementary DNA. (B) Nyquist plots recorded at (a) ssDNA/PANI-MWNT/CHIT/CPE, (b) dsDNA/PANI-MWNT/CHIT/CPE (hybridization with cDNA), (c) the electrode hybridized with ncDNA, (d) the electrode hybridized with one-base mismatched DNA, (e) the electrode hybridized with two-base mismatched DNA. Conditions were the same as in Fig. 3.

technique. The purified PCR product was heated in a water bath at 95 °C for 6 min and then cooled at ice bath to produce the single-stranded DNA sample. The NOS gene probe (namely primer 1) was immobilized onto the PANI-MWNT/CHIT/CPE. Then the NOS gene probe on the electrode was hybridized with the complementary single-stranded DNA sample in the solution. The Nyquist diagrams of $[Fe(CN)_6]^{3-/4-}$ at the PANI-MWNT/CHIT/CPE, the NOS gene probe-immobilized electrode and the hybridized electrode were respectively recorded (see supplementary material, Fig.S6). From the Nyquist diagrams, the R_{et} value was enhanced after immobilizing the NOS gene probe on the PANI-MWNT/CHIT/CPE. After hybridization of the NOS gene probe with the PCR product, the R_{et} value increased obviously. The experimental results indicated that the NOS gene probe-immobilized electrode could successfully recognize and detect the PCR product of the real NOS gene sample.

4. Conclusion

A thin membrane of PANI-MWNT nanocomposites via using a film forming material CHIT was successfully applied to the DNA hybridization sensing. The PANI-MWNT-CHIT organic–inorganic system could exert a synergistic effect on the DNA hybridization detection owing to the superior electron-transfer ability of MWNT and the excellent reversible redox centers of PANI, and resulted in remarkably enhanced electrochemical impedance signal for the DNA hybridization with good regeneration and stability. The transgenes in the transgenic plants could be electrochemically detected with this DNA electrochemical biosensor. The present method demonstrated a promising nanocomposite comprising PANI and MWNT for the construction of bioelectronic devices and biosensors.

Acknowledgements

This work was supported by the National Natural Science Foundation of China (Nos. 20635020, 20805025), Doctoral Foundation of the Ministry of Education of China (No. 20060426001) and Doctoral Fund of QUST (0022278).

Appendix A. Supplementary data

Supplementary data associated with this article can be found, in the online version, at doi:10.1016/j.bios.2008.11.011.

References

Ajayan, P.M., Stephan, O., Colliex, C., Trauth, D., 1994. Science 265, 1212–1214.
Ali, S.R., Ma, Y.F., Parajuli, R.R., Balogun, Y., Lai, W.Y.C., He, H.X., 2007. Anal. Chem. 79, 2583–2587.
Anilkumar, P., Jayakannan, M., 2007. Macromolecules 40, 7311–7319.
Azar, M.H.P., Hejazi, M.S., Alipour, E., 2006. Anal. Chim. Acta 570, 144–150.
Chang, H.X., Yuan, Y., Shi, N.L., Guan, Y.F., 2007. Anal. Chem. 79, 5111–5115.
Feng, Y.Y., Yang, T., Zhang, W., Jiang, C., Jiao, K., 2008. Anal. Chim. Acta, 144–151.
Gao, M., Huang, S.M., Dai, L.M., Wallace, G., Gao, R.P., Wang, Z.L., 2000. Angew. Chem. Int. Ed. 39, 3664–3667.
Gerard, M., Chaubey, A., Malhotra, B.D., 2002. Biosens. Bioelectron. 17, 345–359.
Granot, E., Katz, E., Basnar, B., Willner, I., 2005. Chem. Mater. 17, 4600–4609.
Jiang, C., Yang, T., Jiao, K., Gao, H.W., 2008. Electrochim. Acta 53, 2917–2924.
Kalakodimi, R.P., Nowak, A.M., 2002. Anal. Chem. 74, 5531–5537.
Katz, E., Weizmann, Y., Willner, I., 2005. J. Am. Chem. Soc. 127, 9191–9200.
Lee, K.P., Gopalan, A.I., Lee, S.H., Kim, M.S., 2006. Nanotechnology 17, 375–380.
Li, G.C., Zhang, Z.K., 2004. Macromolecules 37, 2683–2685.
Li, M., Guo, Y., Wei, Y., MacDiarmid, A.G., Lelkes, P.I., 2006. Biomaterials 27, 2705–2715.
Li, A.X., Yang, F., Ma, Y., Yang, X.R., 2007. Biosens. Bioelectron. 22, 1716–1722.
Lu, X.B., Wen, Z.H., Li, J.H., 2006. Biomaterials 27, 5740–5747.
Luo, X.L., Killard, A.J., Smyth, M.R., 2007. Chem. Eur. J. 13, 2138–2143.
Ma, Y.F., Ali, S.R., Dodoo, A.S., He, H.X., 2006a. J. Phys. Chem. B 110, 16359–16365.
Ma, Y.F., Ali, S.R., Wang, L., Chiu, P.L., Mendelsohn, R., He, H.X., 2006b. J. Am. Chem. Soc. 128, 12064–12065.
Nascimento, G.M.D., Corio, P., Novickis, R.W., Temperini, M.L.A., Dresselhaus, M.S., 2005. J. Polym. Sci. A 43, 815–822.
Peng, H., Soeller, C., Travas-Sejdic, J., 2007. Macromolecules 40, 909–914.
Raitman, O.A., Katz, E., Buckmann, A.F., Willner, I., 2002. J. Am. Chem. Soc. 124, 6487–6496.
Rubianes, M.D., Rivas, G.A., 2007. Electrochem. Commun. 9, 480–484.
Sainz, R., Benito, A.M., Martínez, M.T., Galindo, J.F., Sotres, J., Baró, A.M., Corraze, B., Chauvet, O., Maser, W.K., 2005. Adv. Mater. 17, 278–281.
Siqueira, J.R., Gasparotto, L.H.S., Crespilho, F.N., Carvalho, A.J.F., Zucolotto, V., Oliveira, O.N., 2006. J. Phys. Chem. B 110, 22690–22694.
Sorlier, P., Denuziere, A., Viton, C., Domard, A., 2001. Biomacromolecules 2, 765–772.
Virji, S., Huang, J., Kaner, R.B., Weiller, B.H., 2004. Nano Lett. 4, 491–496.
Wei, Z.X., Wan, M.X., Lin, T., Dai, L.M., 2003. Adv. Mater. 15, 136–139.
Xue, H.G., Shen, Z.Q., Li, C.M., 2005. Biosens. Bioelectron. 20, 2330–2334.
Yang, M.H., Yang, Y., Yang, H.F., Shen, G.L., Yu, R.Q., 2006. Biomaterials 27, 246–255.
Yang, G., Hou, W.H., Feng, X.M., Xu, L., Liu, Y.G., Wang, G., Ding, W.P., 2007a. Adv. Funct. Mater. 17, 401–412.
Yang, J., Jiao, K., Yang, T., 2007b. Anal. Bioanal. Chem. 389, 913–921.
Yang, T., Zhang, W., Du, M., Jiao, K., 2008. Talanta 75, 987–994.
Zhang, M.G., Gorski, W., 2005. J. Am. Chem. Soc. 127, 2058–2059.
Zhang, M.G., Smith, A., Gorski, W., 2004. Anal. Chem. 76, 5045–5050.
Zhang, M.N., Gong, K.P., Zhang, H.W., Mao, L.Q., 2005a. Biosens. Bioelectron. 20, 1270–1276.
Zhang, X.T., Lu, Z., Wen, M.T., Liang, H.L., Zhang, J., Liu, Z.F., 2005b. J. Phys. Chem. B 109, 1101–1107.
Zhang, Z.M., Wan, M.X., Wei, Y., 2005c. Nanotechnology 16, 2827–2832.
Zhang, L., Jiang, X., Niu, L., Dong, S.J., 2006. Biosens. Bioelectron. 21, 1107–1115.
Zhou, H.H., Chen, H., Luo, S.L., Chen, J.H., Wei, W.Z., Kuang, Y.F., 2005. Biosens. Bioelectron. 20, 1305–1311.
Zhu, N.N., Chang, Z., He, P.G., Fang, Y.Z., 2006. Electrochim. Acta 51, 3758–3762.
Zou, Y.J., Sun, L.X., Xu, F., 2007. Biosens. Bioelectron. 22, 2669–2674.